Theoretical Investigation of Small Polyatomic Ions Observed in Inductively Coupled Plasma Mass Spectrometry: H_xCO^+ and $H_xN_2^+$ ($x = 1, 2, 3$)

Kyle C. Sears, Jill W. Ferguson,† Timothy J. Dudley,‡ R. S. Houk, and Mark S. Gordon*

Ames Laboratory, U. S. Department of Energy, Department of Chemistry, Iowa State University, Ames, Iowa 50011

Received: September 7, 2007; In Final Form: January 4, 2008

Two series of small polyatomic ions, H_xCO^+ and $H_xN_2^+$ ($x = 1, 2, 3$), were systematically characterized using three correlated theoretical techniques: density functional theory using the B3LYP functional, spin-restricted second-order perturbation theory, and singles + doubles coupled cluster theory with perturbative triples. On the basis of thermodynamic data, the existence of these ions in inductively coupled plasma mass spectrometry (ICP-MS) experiments is not surprising since the ions are predicted to be considerably more stable than their corresponding dissociation products (by 30−170 kcal/mol). While each pair of isoelectronic ions exhibit very similar thermodynamic and kinetic characteristics, there are significant differences within each series. While the mechanism for dissociation of the larger ions occurs through hydrogen abstraction, the triatomic ions (HCO^+ and HN_2^+) appear to dissociate by proton abstraction. These differing mechanisms help to explain large differences in the abundances of HN_2^+ and HCO^+ observed in ICP-MS experiments.

Introduction

Small, hydrogen-containing cations play an important role in numerous areas of chemistry and physics. Organic cations such as the formyl cation (HCO^+) and the formaldehyde cation (H_2CO^+) were among the first polyatomic ions observed in interstellar space.[1] These ions have also been observed in dense clouds associated with formation of stars and gas planets.[2−3] These ions play an important part in hydrocarbon combustion and reactions of O^+ with simple hydrocarbons such as methane.[4] Similar ions, containing nitrogen instead of carbon and oxygen, have been observed in roles that are similar to their organic counterparts. The diazenylium ion (N_2H^+) has been observed in the same type of interstellar media as the formyl cation,[2−3] which is not surprising since they are isoelectronic.

Small polyatomic cations also are prevalent in inductively coupled plasma mass spectrometry (ICP-MS), where atomic ions are preferred for multielement analysis.[5−22] Using a high-temperature (6000 K) atomization source such as an ICP attenuates but often does not completely eliminate many of these undesirable polyatomic ions. These spectral interferences become more troublesome for analysis at the lowest possible concentrations, which is important in key scientific areas such as semiconductor production. Understanding how these ions form could lend insight into how to eliminate their production during an ICP-MS experiment. For example, experimental measurement of the dissociation constant (K_d) associated with a pair of ions can indicate where such ions form, since the constant is a function of temperature. However, the temperature dependence of the constant is determined through use of the partition functions associated with each species involved.[7,23] This in turn requires knowledge of energetic and structural data for each species. Since many polyatomic ions are not very abundant or long-lived, much of this data cannot be easily obtained through experiment. Theoretical calculations offer a solution to such a problem, since they can provide several useful quantities related to partition functions: electronic energies, moments of inertia from stationary geometries, and harmonic vibrational frequencies.

This work focuses on two classes of small polyatomic cations observed in ICP-MS experiments: H_xCO^+ and $H_xN_2^+$ ($x = 1$, 2, 3). Numerous experimental and theoretical studies have been reported for many of these ions, particularly the H_xCO^+ series.[24−39] However, a systematic study of these ions using different levels of theory and basis sets has only been reported for the $x = 1$ triatomic HCO^+ cation[39] and HN_2^+ cation.[40] This work will analyze the thermodynamics and reaction pathways of the ions in each series in order to shed light on the existence of these ions in even the harshest environments. Similarly, analyses involving comparisons between isoelectronic species will be performed in order to understand similarities and differences observed in ICP-MS experiments. Finally, an analysis of the performance of various correlated methods in determining structures and energies of small polyatomic ions will be performed.

Computational Methods

Geometries for all structures were optimized using three methods: density functional theory (DFT) with the B3LYP functional,[41,42] second-order Z-averaged perturbation theory (ZAPT2),[43−46] and singles and doubles coupled cluster theory with perturbative triples, CCSD(T).[47] For open-shell systems, the restricted forms of all of the previously mentioned techniques were used (e.g., RCCSD(T)) The basis set used in all optimizations was the Dunning triple-ζ basis set (TZ)[48] with the Pople (2df,2pd)[49] polarization set included. In this work, this basis set will be referred to as TZ2P(f,d). Frequencies were calculated in order to determine the nature of the stationary points on each potential energy surface (PES). In all cases, the frequencies were

* To whom correspondence should be addressed. E-mail: mark@si.msg.chem.iastate.edu.

† Present address: Materials Science Center, University of Wisconsin—Eau Claire, Eau Claire, WI 54702.

‡ Present address: Department of Chemistry, Villanova University, Villanova, PA 19085.

10.1021/jp077209k CCC: $40.75
Published on Web 03/01/2008

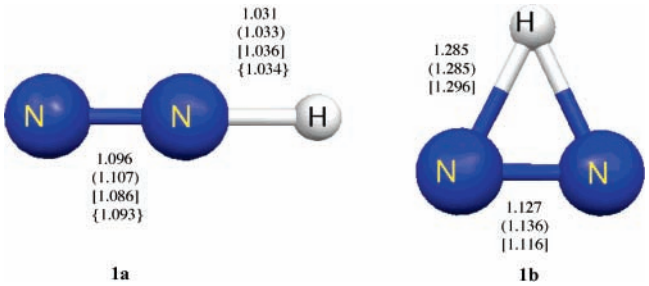

Figure 1. CCSD(T)/TZ2P(f,d) geometries of the diazenylium ion and its transition state associated with hydrogen migration. Values in ( ) are ZAPT2 parameters, and those in [ ] are B3LYP parameters. Experimental values are in { } and were obtained from ref 61. Bond lengths are in angstroms.

calculated by numerically differentiating analytic gradients using a central difference formula. Frequencies at each level of theory can be found in the Supplemental Information. Transition states were connected to their respective minima through intrinsic reaction coordinate (IRC) calculations using the second-order Gonzalez−Schlegel algorithm,[50] with a step size of 0.15 (amu)$^{1/2}$ bohr. IRC calculations were only performed at the B3LYP and ZAPT2 levels of theory. Constrained optimizations using the multiconfigurational self-consistent field (MCSCF) method were used to determine the hydrogen atom/ion abstraction process for each cation considered. Structures along these paths are expected to be configurationally mixed. For singlet structures, the MCSCF active space consisted of two electrons in two orbitals: hydrogen-heavy atom σ and σ^* orbitals. For doublet structures, a similar active space was utilized, except the unpaired electron and corresponding orbital were also included in the active space (three electrons in three orbitals).

Because of the number of low-lying minima on some of the PESs considered, calculations involving a larger basis set were performed to probe the accuracy of the CCSD(T)/TZ2P(f,d) calculations. Single-point energy calculations were performed at each CCSD(T)/TZ2P(f,d) optimized stationary points using the cc-pVQZ basis set. The completely renormalized coupled cluster approach (CR-CC(2,3))[51,52] implemented in GAMESS[53] was used to calculate the energies. This completely renormalized CC approach correctly accounts for diradical character (near degeneracies) and is therefore better able than traditional CCSD(T) to account for nondynamic correlation effects. All B3LYP, ZAPT2, MCSCF, and CR-CC(2,3) calculations were performed using GAMESS, and all CCSD(T) calculations were performed using ACES II.[54] Default tolerances were used in all geometry optimizations and frequency calculations.

Results

N_2H^+. The diazenylium ion (N_2H^+) has been previously characterized both theoretically[40,55−59] and experimentally.[58−63] Figure 1 shows the structures and optimized geometrical parameters for both stationary points associated with the ground state N_2H^+ cation. The linear structure (1a) is the potential energy minimum, and the ring structure (1b) is the transition state associated with proton transfer between the two nitrogen atoms. The B3LYP N−N bond lengths calculated for both structures in Figure 1 are about 0.01 Å shorter than the CCSD(T) distances, while the ZAPT2 distances are about 0.01 Å too long. The N−H bond length for the N_2H^+ minimum agrees to within 0.005 Å at all levels of theory, whereas the B3LYP N−H bond length in the transition-state structure (1b) is 0.011 Å longer than that determined at the CCSD(T) and ZAPT2 levels of theory. The present calculations agree quite well (within 0.003 Å for all bond lengths) with previously reported geometries at the CCSD(T)/aug-cc-pVXZ (x = T, Q) and MC-QCISD/6-31G(d,p) levels of theory.[55,57]

TABLE 1: Relative Energies of Stationary Points and Dissociation Limits Associated with N_2H^+ (Energies Are in kcal/mol)

	1a	1b	$N_2 + H^+$	$N_2^+ + H$
B3LYP/TZ2P(f,d)	0	48.9	123.5	179.0
ZAPT2/TZ2P(f,d)	0	51.2	123.1	160.3
CCSD(T)/TZ2P(f,d)	0	49.9	125.3	171.7
CR-CC(2,3)/cc-pVQZ[a]	0	49.0	123.7	167.4

[a] Energy evaluated at CCSD(T)/TZ2P(f,d)-optimized geometry.

Table 1 lists the relative energies calculated at various levels of theory for the structures on the ground-state PES of N_2H^+. At all levels of theory, the diazenylium ion is calculated to be considerably lower in energy than the lowest two dissociation limits involving abstraction of the hydrogen moiety (either as a proton or hydrogen atom). Excellent agreement among the methods is observed for the dissociation energy involving proton abstraction (within 2 kcal/mol relative to coupled-cluster energies). However, the agreement is worse for the hydrogen abstraction process, with the ZAPT2 dissociation energy being 11.4 kcal/mol lower than the CCSD(T) value and the B3LYP energy being 7.3 kcal/mol higher. The CCSD(T) dissociation energy for this process is 4.3 kcal/mol higher than the CR-CC/cc-pVQZ energy. This notable difference in the dissociation energy associated with hydrogen atom abstraction is primarily due to differences in the Hartree−Fock (HF) energies of the hydrogen atom using different basis sets (4.2 kcal/mol) and *not* due to inadequacies of the basis set in calculating correlation energy. A trend is observed (vide infra) in which the CCSD(T)/TZ2P(f,d) energies agree quite well with the CR-CC/cc-pVQZ energies (within 1.6 kcal/mol) except for dissociation limits involving hydrogen atom abstraction. However, the CCSD(T) calculations consistently overestimate these limits by 3.3−4.3 kcal/mol with respect to the CR-CC values, which is close to the difference in the HF energies of the hydrogen atom using the two basis sets. Since the CCSD(T)/TZ2P(f,d) calculations appear to adequately describe the correlation energy of these polyatomic cations, the energies of the B3LYP and ZAPT2 calculations will be compared directly to the CCSD(T) energies. Such a comparison should be more insightful and consistent since all three methods utilize the same basis set.

The experimental[64] energy difference between the two dissociation limits analyzed in Table 1 is 46.1 kcal/mol. From Table 1, one can see that the coupled cluster energy differences are quite good (46.4 kcal/mol for CCSD(T) and 43.7 kcal/mol for CR-CC), while ZAPT2 significantly underestimates the difference (37.2 kcal/mol) and B3LYP overestimates the difference by a similar margin (55.5 kcal/mol). Note that the vibrational zero point energy (ZPE) correction was not included in these calculations and would only have a small effect on the differences (<0.3 kcal/mol). The CCSD(T) transition state corresponding to hydrogen atom transfer from one nitrogen atom to the other in the diazenylium ion is predicted to be 49.9 kcal higher in energy than the associated minima. The other methods predict a similar value.

Note that the calculations indicate that the preferred pathway for dissociation of N_2H^+ is proton loss to N_2 and H^+. However, the ICP-MS experiments measure the abundance ratio N_2^+/N_2H^+ and use an estimate for the number density of hydrogen atoms in the ICP.[65] Although a peak can be measured for H^+ from the ICP, it is not easy to estimate the sensitivity of the MS at m/z 1, since there are no nearby metal ions to use as mass bias calibrants.

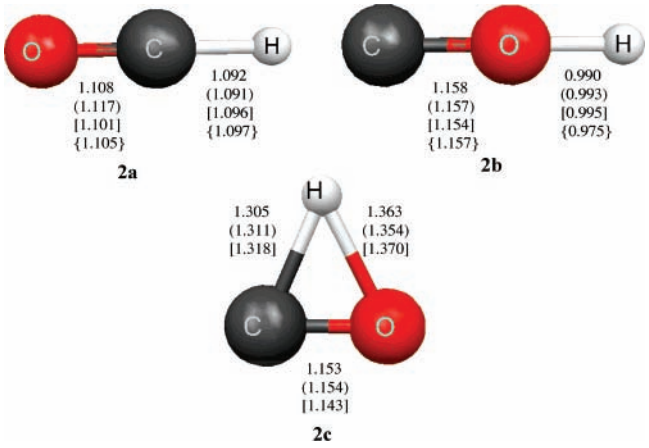

Figure 2. CCSD(T)/TZ2P(f,d) geometries of the formyl and isoformyl cations along with that of the associated transition state. Values in ( ) are ZAPT2 parameters, and those in [ ] are B3LYP parameters. Experimental values are in { } and were obtained from refs 68, 73, and 81. Bond lengths are in angstroms.

TABLE 2: Relative Energies of Stationary Points and Dissociation Limits Associated with COH^+ (Energies Are in kcal/mol)

	2a	2b	2c	$CO + H^+$	$CO^+ + H$
B3LYP/TZ2P(f,d)	0	38.7	76.7	147.2	164.8
ZAPT2/TZ2P(f,d)	0	46.4	81.5	150.2	160.3
CCSD(T)/TZ2P(f,d)	0	40.4	77.4	149.1	159.6
CR-CC(2,3)/cc-pVQZ[a]	0	39.5	76.5	147.6	155.3

[a] Energy evaluated at CCSD(T)/TZ2P(f,d)-optimized geometry.

HCO^+. The formyl cation (HCO^+) has been characterized extensively using experimental[66−73] and theoretical[39,74−77] techniques. The isoformyl cation (COH^+) has received less attention, particularly in experimental studies.[78−81] Figure 2 shows the optimized structures for both the formyl (2a) and isoformyl (2b) cations, along with the transition state corresponding to H-atom transfer between the two structures (2c). The C−O bond length in the formyl cation is predicted to be 0.009 Å longer at the ZAPT2 level and 0.007 Å shorter at the B3LYP level than that calculated at the CCSD(T) level of theory (1.108 Å). The C−H bond length agrees quite well among the different calculations (within 0.005 Å). Similarly, the isoformyl cation O−H bond lengths agree quite well (within 0.005 Å) among the three methods. The C−O bond lengths determined at each level of theory exhibit even better agreement (within 0.003 Å). The C−H and O−H bond lengths calculated at the various levels agree to within 0.01 Å in almost all cases with the B3LYP C−H bond length being the only exception. Geometries determined at each level of theory agree quite well with experimentally determined geometries. The only exception is the O−H bond in the isoformyl cation, which is overestimated by at least 0.015 Å at all levels of theory. This result is not unexpected based on previous studies of this system by Schaefer et al.[39] The very low frequency bending vibration associated with this molecule is believed to be the reason for the discrepancies between theory and experiment for this system.

Table 2 lists the relative energies of the various stationary points on the ground-state PES of COH^+ along with the lowest two dissociation limits associated with abstracting the hydrogen atom or the proton from the C−O fragment. Both the formyl and isoformyl cations are quite stable compared to either dissociation limit shown in Table 2, with the formyl cation being more stable by 40.4 kcal/mol at the CCSD(T) level. The B3LYP and CCSD(T) relative energy differences between the two minima are in good agreement, whereas ZAPT2 is off by ~6.0 kcal/mol. Similarly, the B3LYP and CCSD(T) isomerization barriers leading from the formyl cation agree to within 1 kcal/mol, while the ZAPT2 value is too high by 4.1 kcal/mol. The predicted dissociation energy for proton abstraction agrees quite well among all of the methods (within 2.5 kcal/mol), with the CCSD(T) dissociation energy calculated to be 149.1 kcal/mol. The ZAPT2 and CCSD(T) dissociation energies for hydrogen atom abstraction agree to within 1 kcal/mol, while B3LYP overestimates this dissociation energy by about 5 kcal/mol. The coupled cluster dissociation energies (10.5 and 7.7 kcal/mol for CCSD(T) and CR-CC, respectively) are in reasonable agreement with the experimental[64] value of 9.2 kcal/mol. The ZAPT2 dissociation energy difference (10.1 kcal/mol) also agrees well with the experimental value, while B3LYP is off by nearly a factor of 2 (17.6 kcal/mol).

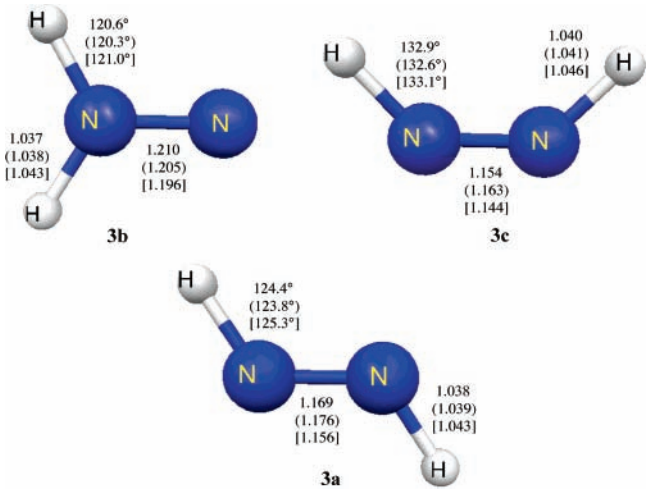

Figure 3. CCSD(T)/TZ2P(f,d) geometries of the *iso*-, *cis*-, and *trans*-diazene cations. Values in ( ) are ZAPT2 parameters, and those in [ ] are B3LYP parameters. Bond lengths are in angstroms.

$H_2N_2^+$. Figure 3 shows the structures and geometrical parameters of the three low-lying minima on the ground-state PES for $H_2N_2^+$. The N−H bond lengths for all structures in Figure 3 are nearly identical regardless of the level of theory. The spread in the predicted N−N bond length in *trans*-diazene cation (3a) is larger, ~0.02 Å, with CCSD(T) in the middle (1.169 Å), ZAPT2 too long, and B3LYP too short. All levels of theory predict a decrease in the N−N bond length (by 0.012−0.015 Å) in the *cis*-diazene (3c) cation relative to the trans structure. There is considerable elongation of the N−N bond in the *iso*-diazene (3b) cation compared to both the trans and cis structures. Few theoretical calculations have been reported for these systems, with some discrepancies existing among various interpretations of the PES. The present calculations, in agreement with earlier lower-level studies by Pople and Curtiss,[82] indicate that there are three local minima on the ground-state PES. Recent RCCSD[T] calculations by Palaudoux and Hochlaf[83] suggest that the cis structure is actually a saddle point and that two other nonplanar minima exist on the ground-state surface.

Figure 4 shows the structures for two transition states that correspond to isomerizations between pairs of minima on the ground state PES of $H_2N_2^+$. The hydrogen-bridging structure (3d) corresponds to the transition state between the *trans*- and *iso*-diazene cations. Neither ZAPT2 nor B3LYP is in consistently good agreement with the CCSD(T) geometries. Much closer agreement is seen for the second transition state that is associated with the isomerization between the *cis*- and *trans*-diazene ions (3e).

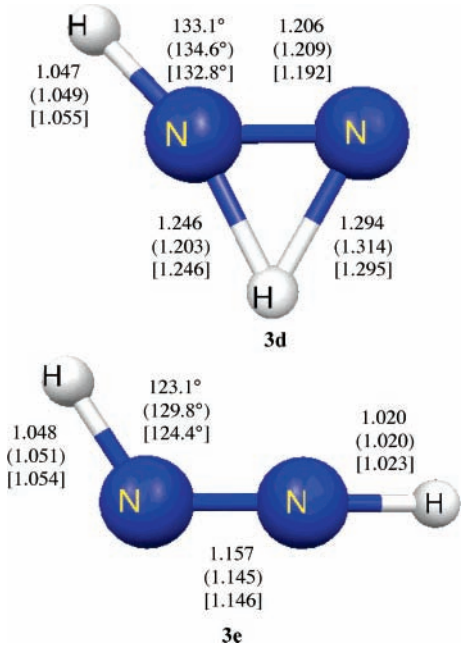

Figure 4. CCSD(T)/TZ2P(f,d) geometries of the transition states associated with *trans*-/*iso*-diazene cation isomerization and *trans*-/*cis*-diazene cation isomerization. Values in ( ) are ZAPT2 parameters, and those in [ ] are B3LYP parameters. Bond lengths are in angstroms.

TABLE 3: Relative Energies of Stationary Points and Dissociation Limits Associated with $N_2H_2^+$ (Energies Are in kcal/mol)

	3a	3b	3c	3d	3e	$N_2H^+ + H$	$N_2H + H^+$
B3LYP/TZ2P(f,d)	0	3.1	5.9	55.8	13.5	47.8	164.3
ZAPT2/TZ2P(f,d)	0	10.6	6.4	56.8	17.2	37.6	170.0
CCSD(T)/TZ2P(f,d)	0	1.5	6.5	54.0	14.2	39.3	165.2
CR-CC(2,3)/cc-pVQZ[a]	0	1.5	6.4	53.6	14.4	36.0	163.7

[a] Energy evaluated at CCSD(T)/TZ2P(f,d)-optimized geometry.

Table 3 lists the relative energies of all previously described stationary points on the ground-state $H_2N_2^+$ PES. All three minima are relatively close in energy, and all levels of theory predict the *trans*-diazene ion to be the global minimum. All methods are generally in excellent agreement with each other, except ZAPT2 predicts a relative energy for the *iso*-diazene ion (3b) that is much too high. This leads to an incorrect prediction that the *cis*-diazene ion (3c) is more stable than the *iso*-diazene ion, in disagreement with both coupled cluster and B3LYP, as well as with earlier G2 calculations by Pople and Curtiss.[82] The 14.2 kcal/mol CCSD(T) barrier to isomerization between the cis and trans isomers (3e) is in good agreement with the B3LYP barrier, while ZAPT2 overestimates the barrier by 3.0 kcal/mol. The CCSD(T) isomerization barrier connecting the iso and trans isomers (3d) is much higher in energy, 54.0 kcal/mol, with similar values predicted by both B3LYP and ZAPT2. The CCSD(T) dissociation limit corresponding to the removal of a hydrogen atom from $N_2H_2^+$ is only 39.3 kcal/mol higher in energy than the global minimum (3a). While ZAPT2 predicts a similar result, B3LYP overestimates the dissociation energy by 8.5 kcal/mol. Removal of a proton from $N_2H_2^+$ requires much more energy (>100 kcal/mol) than hydrogen atom abstraction. Experimentally,[84] the difference between the two dissociation limits was determined to be 133.8 kcal/mol. The CCSD(T) calculations predict the difference to be 125.9 kcal/mol, underestimating the difference by ~8 kcal/mol with the CR-CC calculations being in slightly better agreement (127.7 kcal/mol) with experiment. The B3LYP calculations underestimate the difference by 17.2 kcal/mol, more than twice that of the CCSD(T) calculation. Interestingly, the ZAPT2 energy difference is much closer to the experimental value than the B3LYP and coupled-cluster calculations (132.4 kcal/mol).

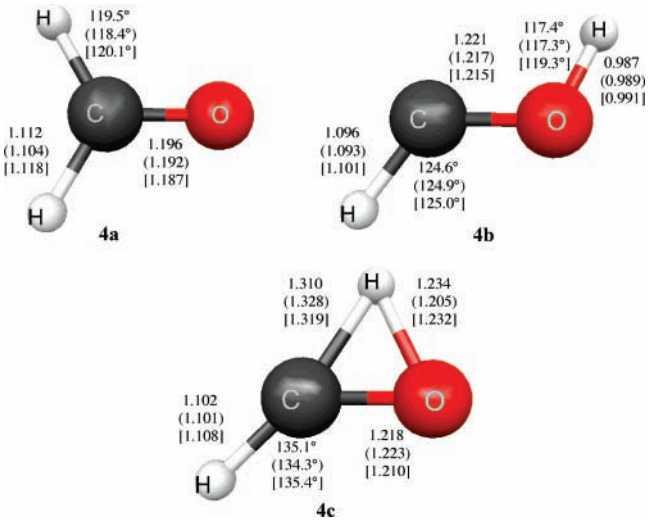

Figure 5. CCSD(T)/TZ2P(f,d) geometries of the formaldehyde and hydroxymethylene cations along with the associated transition state. Values in ( ) are ZAPT2 parameters, and those in [ ] are B3LYP parameters. Bond lengths are in angstroms.

TABLE 4: Relative Energies of Stationary Points and Dissociation Limits Associated with H_2CO^+ (Energies Are in kcal/mol)

	4a	4b	4c	$HCO^+ + H$	$HCO + H^+$
B3LYP/TZ2P(f,d)	0	5.4	47.3	39.6	157.8
ZAPT2/TZ2P(f,d)	0	−3.1	33.4	15.9	146.2
CCSD(T)/TZ2P(f,d)	0	5.4	45.9	31.8	158.5
CR-CC(2,3)/cc-pVQZ[a]	0	5.0	45.5	28.5	157.2

[a] Energy evaluated at CCSD(T)/TZ2P(f,d)-optimized geometry.

H_2CO^+. The formaldehyde cation (4a) and hydroxymethylene cation (4b) have been previously characterized through numerous experimental[24−29] and theoretical[30−38] studies, particularly the formaldehyde cation. Figure 5 shows the structures and geometrical parameters calculated for the two minima and the associated transition state (4c) on the ground state H_2CO^+ PES. In general ZAPT2 underestimates bond distances relative to CCSD(T), and B3LYP overestimates them, but all three levels of theory are in reasonable agreement. In the transition state, the ZAPT2 O−H and C−H bond lengths that are associated with the bridging hydrogen are considerably different from those predicted by both CCSD(T) and B3LYP, which agree quite closely with one another. The ZAPT2 O−H bond length is nearly 0.030 Å shorter, and the C−H bond length is nearly 0.02 Å longer.

Table 4 lists the relative energies of the various stationary points on the H_2CO^+ PES, including two related dissociation limits. The most noticeable trend in this table is the severe underestimation of relative energies at the ZAPT2 level of theory. While CCSD(T) and B3LYP predict the formaldehyde cation to be the global minimum and the hydroxymethylene cation to be about 5 kcal/mol higher in energy, ZAPT2 predicts the hydroxymethylene cation to be about 3 kcal/mol *lower* in energy. This inability of perturbation theory to correctly predict the relative energies of these structures is well documented, despite the fact that the geometries are in good agreement with those obtained from higher-level calculations. ZAPT2 also underestimates the relative energies of the transition state and

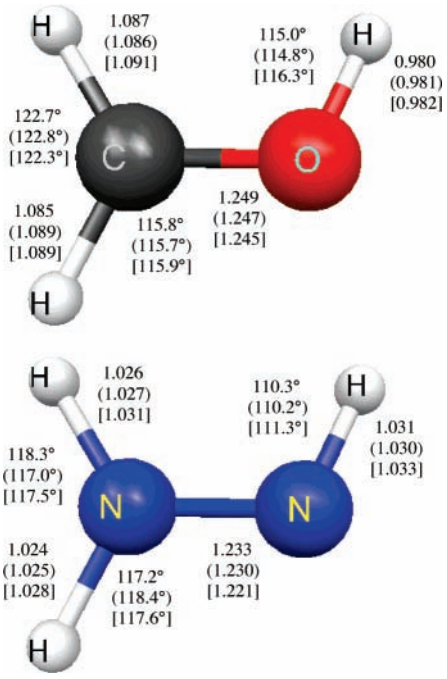

Figure 6. CCSD(T)/TZ2P(f,d) geometries of the global minimum on the H_3CO^+ and $H_3N_2^+$ PESs. Values in ( ) are ZAPT2 parameters, and those in [ ] are B3LYP parameters. Bond lengths are in angstroms.

both dissociation limits by 10−16 kcal/mol. This is a rather large error, considering the CCSD(T) relative energy for the transition state is only 45.9 kcal/mol and that for the lowest dissociation limit is 31.8 kcal/mol. B3LYP relative energies are in relatively good agreement with the CCSD(T) results, particularly for the bound structures. B3LYP overestimates the dissociation energy for the lowest dissociation limit by almost 8 kcal/mol compared to the CCSD(T) value but agrees well with the CCSD(T) value for the higher dissociation limit. The energy difference between the dissociation limits at the coupled cluster levels (126.7 and 128.7 kcal/mol for CCSD(T) and CR-CC, respectively) compare quite well to the experimental value[84] of 126.4 kcal/mol. The ZAPT2 calculations overestimate this difference by almost 4 kcal/mol, while the B3LYP calculations underestimate the value by just over 8 kcal/mol.

$H_3N_2^+$ and H_3CO^+. The triplet methoxy cation has been extensively studied due to its reactivity through nonadiabatic processes.[85−88] On the basis of preliminary calculations, this structure and the isoelectronic triplet dinitrogen species were not considered in this work since these ions are considerably higher in energy (>50 kcal/mol) than the corresponding global minima and are probably not important in the relevant experiments (i.e., in an ICP at $T \approx 6000$ K). Figure 6 depicts the geometries for the global minimum structures for the $H_3N_2^+$ and H_3CO^+ singlet cations, which are both planar. Although these structures are considerably more stable than their triplet counterparts, few calculations on these species have been reported.[37,89−91] The ZAPT2 and B3LYP geometrical parameters for the H_3N_2 singlet cation agree quite well with the CCSD(T) values. Most bond lengths agree to within 0.005 Å, and the angles agree to within 1°. Similar comments apply to the H_2COH^+ singlet cation; all bond lengths agree to within 0.004 Å of the CCSD(T) result, and most bond angles agree to within 1°. Attempts to find nonplanar minima comparable in energy to the ground-state minima (within 50 kcal/mol) for both ions were unsuccessful.

Table 5 lists the relative energies of the dissociation limits associated with $H_3N_2^+$ at various levels of theory. The abstraction of a hydrogen atom from $H_3N_2^+$ requires a large amount of energy (∼100 kcal/mol), with the proton abstraction process requiring approximately twice as much energy. The B3LYP and CCSD(T) relative energies agree quite well (within 2 kcal/mol), while the ZAPT2 energies deviate from the CCSD(T) values by ∼2−8 kcal/mol. Table 6 lists the energies of the dissociation limits associated with the H_2COH^+ cation at the same levels of theory. Qualitatively the energies are similar to those for the nitrogen-containing analog: hydrogen abstraction requires a large amount of energy (at least 100 kcal/mol), and the corresponding proton abstraction process requires considerably more energy (>50 kcal/mol).

TABLE 5: Relative Energies of Stationary Points and Dissociation Limits Associated with $H_3N_2^+$ (Energies Are in kcal/mol; B3LYP, ZAPT2, and CCSD(T) Energies Calculated Using TZ2P(f,d) Basis Set)

	B3LYP	ZAPT2	CCSD(T)	CR-CC(2,3)/cc-pVQZ[a]
$H_3N_2^+$	0	0	0	0
(*trans*) $H_2N_2^+ + H$	104.1	96.1	104.0	100.3
(*iso*) $H_2N_2^+ + H$	107.2	106.7	105.5	101.8
(*cis*) $H_2N_2^+ + H$	110.0	102.5	110.5	106.7
(*trans*) $H_2N_2 + H^+$	193.6	191.7	194.0	193.1
(*cis*) $H_2N_2 + H^+$	199.1	197.6	199.5	198.4
(*iso*) $H_2N_2 + H^+$	215.8	220.3	219.9	218.3

[a] Energy evaluated at CCSD(T)/TZ2P(f,d)-optimized geometry.

TABLE 6: Relative Energies of Stationary Points and Dissociation Limits Associated with H_3CO^+ (Energies Are in kcal/mol; B3LYP, ZAPT2, and CCSD(T) Energies Calculated Using TZ2P(f,d) Basis Set)

	B3LYP	ZAPT2	CCSD(T)	CR-CC(2,3)/cc-pVQZ[a]
H_3CO^+	0	0	0	0
$H_2CO^+ + H$	119.5	127.0	119.2	115.8
$HCOH^+ + H$	124.9	123.9	124.6	120.8
$H_2CO + H^+$	178.3	176.9	179.4	178.4
$HCOH + H^+$	230.6	232.3	230.8	230.1

[a] Energy evaluated at CCSD(T)/TZ2P(f,d)-optimized geometry.

Discussion

Since the HCO^+ and N_2H^+ cations are isoelectronic, one expects that they will have similar thermodynamic and kinetic parameters. Tables 1 and 2 show that the thermodynamic stabilities of these species compared with their respective dissociation limits are both quite large (>120 kcal/mol). Despite the similarities in the thermodynamics associated with these two ions, ICP-MS experiments[65] have shown that the abundance ratios N_2^+/CO^+ and N_2H^+/HCO^+ are about four and ten, respectively. While thermodynamic arguments can explain the abundance of N_2H^+ compared to N_2^+, it provides no insight into the differences between the two isoelectronic species. The ionization energies of neutral N_2H and HCO are in the range 7.8 to 8.2 eV[84] close enough that differences in the extent of ionization are unlikely to be responsible for the different abundances of N_2H^+ and HCO^+.

Examination of the mechanisms for dissociation of HCO^+ and N_2H^+ does give an indication of why there are different abundances of these ions. Simple MCSCF calculations reveal that these ions dissociate smoothly into a neutral diatomic molecule and a proton when they are pulled apart. These dissociation limits are also significantly lower in energy than the corresponding hydrogen abstraction processes. Thus, the association of the neutral diatomic molecule and a proton within the experimental apparatus could lead to higher than expected

levels of the triatomic cations. The higher abundance of N_2H^+ than HCO^+ in the mass spectrum may thus be related to different abundances of the corresponding neutral N_2 and CO in the ICP.

The thermodynamics of H_2CO^+ and $N_2H_2^+$ exhibit numerous similarities as expected. The minima on each surface are more thermodynamically stable than the dissociation products but not nearly to the extent seen for the triatomic cations described above. The one significant difference between these two systems is that no minimum corresponding to a *cis*-like species was found for H_2CO^+. Each PES exhibits multiple minima that are relatively close in energy: H_2CO^+ has two minima within 6 kcal/mol of each other, and $N_2H_2^+$ has three minima within a 7 kcal/mol range. Despite these closely spaced minima, the PESs are not shallow and featureless. Relatively large barriers (45−55 kcal/mol) corresponding to hydrogen transfer between heavy atoms exist on both PESs. On the $N_2H_2^+$ surface, a considerably smaller barrier (14 kcal/mol) was found leading to isomerization between the cis and trans isomers. The dissociation pathways for the formaldehyde cation and the *iso*-diazene ion were found to be similar in that they both dissociate to form a hydrogen atom and the corresponding triatomic cation (HCO^+ or HN_2^+). This is significantly different than the mechanism found for the triatomic cations themselves, which appear to form through protonation of a neutral diatomic molecule rather than through a radical reaction involving a hydrogen atom and a diatomic cation. Similarly, the dissociation of the *trans*-diazene ion leads to the hydrogen atom and N_2H^+. Thus, the formation of both the H_2CO^+ and $N_2H_2^+$ cations appears to be dependent on the concentration of hydrogen atoms and HCO^+ and N_2H^+ cations.

Though the singlet H_2COH^+ and $H_3N_2^+$ cations appear to be global minima, few calculations have been reported for these structures. The two structures are very similar in many respects. They both have planar geometries and are very stable with respect to the lowest dissociation limits (about 100 kcal/mol). MCSCF calculations show that dissociation of the hydroxy hydrogen in H_2COH^+ leads to the formation of a hydrogen atom and the formaldehyde cation. The similar process for $H_3N_2^+$ leads to formation of a hydrogen atom and the *iso*-diazene cation. The abstraction of a hydrogen from $H_3N_2^+$ to form a translike species results in the removal of a hydrogen atom to form the *trans*-diazene cation. These processes more closely resemble the dissociations of the tetra-atomic cations as opposed to the triatomic cations.

The biggest discrepancy between geometries using different methods was observed for the transition states involving a bridged hydrogen. The ZAPT2 hydrogen-heavy atom bond lengths involving the bridging hydrogen are often significantly different from the B3LYP and CCSD(T) values. These differences are usually larger than 0.01 Å and as high as 0.03 Å. The B3LYP distances generally agree to within 0.01 Å with the CCSD(T) values. The ZAPT2 relative energies are often considerably different from those determined at the CCSD(T) level of theory; in some cases (H_2CO^+ and $H_2N_2^+$) ZAPT2 predicts incorrect energy ordering for the minima. In most cases, the B3LYP energies agree very well with the CCSD(T) results and predict the correct ordering of minima for all structures. The effect of the basis set has a minimal role in determining the energetics of the small polyatomic cations considered. The TZ2P(f,d) basis set appears to be adequate in determining the correlation energy of the species considered. However, the inadequacies of this basis set in determining the HF energy of the hydrogen atom did show significant, though predictable, differences in the energies associated with hydrogen atom abstraction processes. Analysis of the T1 amplitudes from the CR-CC single-point calculations indicates that essentially all of the structures analyzed have very little multireference character, including transition-state structures. The one exception is the formaldehyde cation, which does exhibit some multireference character (largest T1 amplitude = −0.154). This fact could explain the difficulty perturbation theory has in determining the proper energy ordering of the formaldehyde and hydroxymethylene cations.

It appears that geometries are not very sensitive to the choice of method used. This is good news for the intended fundamental studies of polyatomic ions in ICP-MS as a reasonable estimate of the geometry is probably sufficient to allow calculation of the vibrational and rotational partition functions. Also, larger systems similar to the ones studied in this work could be accurately probed using relatively simple correlated methods to obtain geometries. However, one must be cautious of using perturbative methods to obtain relative energies, as the dissociation constant is highly temperature sensitive.

Conclusions

Two series of small polyatomic ions, H_xCO^+ and $H_xN_2^+$ (x = 1, 2, 3), were systematically characterized using CCSD(T), ZAPT2, and B3LYP. Despite a large difference in the abundances of HCO^+ and HN_2^+ in recent ICP-MS experiments, these isoelectronic ions are found to have similar dissociation energies and pathways based on theoretical calculations. Each pathway corresponds to deprotonation of the ion to form a neutral diatomic molecule. This observation could explain the concentration differences since the experiments were performed under atmospheric conditions. Also, protonation of the diatomic molecules leads to a much more thermodynamically stable species (>120 kcal/mol). For the tetra-atomic species, H_2CO^+ and $H_2N_2^+$, both the thermodynamics and kinetics differ significantly from the triatomic ions. The dissociation pathway associated with these species corresponds to hydrogen atom abstraction leading to the previously mentioned triatomic cation. Though formation of the tetra-atomic cations leads to more thermodynamically stable structures, the difference in energy between these structures and their dissociation limits (<40 kcal/mol) is much smaller than for the triatomic/diatomic systems. One significant difference observed between these two isoelectronic species is the absence of a *cis*-like stationary point on the H_2CO^+ PES.

The H_3CO^+ and $H_3N_2^+$ cations are very similar in that they both are roughly 100 kcal/mol more stable than their dissociation products. The dissociation products for these structures are a hydrogen atom and the corresponding tetra-atomic cation. For each series, the formation of the larger polyatomic cation is energetically favored by a considerable amount, though this value differs significantly depending on the ion formed. Thus, it is not surprising that such ions are detected in experiments in which even a "complete" atomization source, such as an ICP, is used. The primary difference within each series is that the formation of the triatomic ion is through a protonation process rather than through addition of a hydrogen atom, which may be why HCO^+ and HN_2^+ are present at very different abundances in ICP-MS experiments.

An analysis of the reliability of the three methods used for predicting geometries and relative energies suggests that B3LYP and ZAPT2 geometries typically agree well with those determined at the CCSD(T) level of theory. The ZAPT2 calculations have more difficulty predicting the geometries of transition states that involve a bridging hydrogen. Relative energies determined at the ZAPT2 level are in many cases in relatively poor

agreement with CCSD(T) values, while B3LYP energies are typically in good agreement. On the basis of T1 amplitudes generated at the CR-CC(2,3)/cc-pVQZ level and the very small differences between the CR-CC and CCSD(T) energies, there is very little multireference character in the cations considered. Therefore, using simple correlated methods to predict geometries for such systems appears to be a reasonable approach, though energy calculations are very sensitive to the method used and must be analyzed carefully.

Acknowledgment. This work was supported by National Science Foundation, Analytical and Surface Chemistry Program, Grant No. 0309381. K.S. was supported in part by a National Science Foundation REU grant and in part by funds generously provided by the ISU chemistry department.

Supporting Information Available: B3LYP, ZAPT2, and CCSD(T) vibrational frequencies for all stationary points reported in this work are included. This material is available free of charge via the Internet at http://pubs.acs.org.

References and Notes

(1) Buhl, D.; Snyder, L. E. *Nature* **1970**, *228*, 267−269.
(2) Caselli, P.; Myers, P. C.; Thaddeus, P. *Astrophys. J.* **1995**, *455*, L77.
(3) Ziurys, L. M.; Apponi, A. J. *Astrophys. J.* **1995**, *445*, L73.
(4) Warnatz, J. In *Combustion Chemistry*; Gardiner, W. C., Jr., Ed.; Springer-Verlag: Berlin, 1984; 197−360.
(5) Houk, R. S.; Fassel, V. A.; Flesch, G. D.; Svec, H. J.; Gray, A. L.; Taylor, C. E. *Anal. Chem.* **1980**, *52*, 2283−2289.
(6) Niu, H.; Houk, R. S. *Spectrochim. Acta, Part B* **1996**, *51*, 779−815.
(7) Houk, R. S.; Praphairaksit, N. *Spectrochim. Acta, Part B* **2001**, *56*, 1069−1096.
(8) Taylor, V. F.; March, R. E.; Longerich, H. P.; Stadey, C. J. *Int. J. Mass Spectrom.* **2005**, *243*, 71−84.
(9) Nonose, N. S.; Matsuda, N.; Fudagawa, N.; Kubota, M. *Spectrochim. Acta, Part B* **1994**, *49*, 955−974.
(10) Tanner, S. D. *J. Anal. At. Spectrom.* **1995**, *10*, 905−921.
(11) Tanner, S. D.; Baranov, V. I.; Bandura, D. R. *Spectrochim. Acta, Part B* **2002**, *57*, 1361−1452.
(12) Nonose, N.; Kubota, M. *J. Anal. At. Spectrom.* **2001**, *16*, 551−559.
(13) Nonose, N.; Kubota, M. *J. Anal. At. Spectrom.* **2001**, *16*, 560−566.
(14) Nonose, N. *J. Mass Spectrom. Soc. Jpn.* **1997**, *45*, 77−89.
(15) Tanner, S. D. *J. Anal. At. Spectrom.* **1993**, *8*, 891−897.
(16) Becker, J. S.; Dietze, H.-J. *J. Anal. Chem.* **1997**, *359*, 338−345.
(17) Evans, E. H.; Ebdon, L.; Rowley, L. *Spectrochim. Acta Part B* **2002**, *57*, 741−754.
(18) Fraser, M. M.; Beauchemin, D. *Spectrochim. Acta Part B* **2001**, *56*, 2479−2495.
(19) Holliday, A. E.; Beauchemin, D. *J. Anal. At. Spectrom.* **2003**, *18*, 289−295.
(20) Guenther, D.; Longerich, H. P.; Jackson, S. E.; Forsythe, L. *J. Anal. Chem.* **1996**, *355*, 771−773.
(21) Zahran, N. F.; Helal, A. I.; Amr, M. A.; Abdel-Hafiez, A.; Mohsen, H. T. *Int. J. Mass Spectrom.* **2005**, *226*, 271−278.
(22) Reed, N. M.; Cairns, R. O.; Hutton, R. C.; Takaku, Y. *J. Anal. At. Spectrom.* **1994**, *9*, 881−896.
(23) Houk, R. S. *Spectrochim. Acta, Part B* **2006**, *61*, 235−236.
(24) Dalgarno, A.; Black, J. H. *Rep. Prog. Phys.* **1976**, *39*, 573−612.
(25) Smith, D.; Adams, N. G. *Astrophys. J.* **1977**, *217*, 741.
(26) Huntress, W. T. *Astrophys. J. Suppl. Ser.* **1977**, *33*, 495.
(27) Bohme, D. K.; Goodings, J. M.; Ng, C.-W. *Int. J. Mass Spectrom.* **1977**, *24*, 335.
(28) Liu, J.; Van Devener, B.; Anderson, S. L. *J. Chem. Phys.* **2003**, *119*, 200−214.
(29) Liu, J.; Anderson, S. L. *J. Chem. Phys.* **2004**, *120*, 8528−8536.
(30) Ma, N. L.; Smith, B. J.; Collins, M. A.; Pople, J. A.; Radom, L. *J. Phys. Chem.* **1989**, *93*, 7759−7760.
(31) Takeshita, K. *J. Chem. Phys.* **1991**, *94*, 7259−7265.
(32) Cesar, A.; Ågren, H.; Helgaker, T.; Jørgensen, P.; Jensen, H. J. A. *J. Chem. Phys.* **1991**, *95*, 5906−5917.
(33) Ma, N. L.; Radom, L.; Collins, M. A. *J. Chem. Phys.* **1992**, *96*, 1093−1104.
(34) Ma, N. L.; Smith, B. J.; Radom, L. *Chem. Phys. Lett.* **1992**, *193*, 386−394.
(35) Nguyen, M. T.; Creve, S.; Vanquickenborne, L. G. *J. Phys. Chem.* **1996**, *100*, 18422−18425.
(36) Francisco, J. S.; Thoman, J. W. *Chem. Phys. Lett.* **1999**, *300*, 553−560.
(37) Francis, G. J.; Wilson, P. F.; Maclagan, R. G. A. R.; Freeman, C. G.; Meot-Ner, M.; McEwan, M. J. *J. Phys. Chem. A* **2004**, *108*, 7548−7553.
(38) Levandier, D. J.; Chiu, Y.−H.; Dressler, R. A.; Sun, L.; Schatz, G. C. *J. Phys. Chem. A* **2004**, *108*, 9794−9804.
(39) Yamaguchi, Y.; Richards, C. A.; Schaefer, H. F. *J. Chem. Phys.* **1994**, *101*, 8945-8954.
(40) Sheng, Y.; Leszczynski, J. *J. Chem. Phys. A* **2002**, *106*, 12095−12102.
(41) Becke, A. *J. Chem. Phys.* **1993**, *98*, 5648−5652.
(42) Lee, C. T.; Yang, W. T.; Parr, R. G. *Phys. Rev. B: Condens. Matter* **1988**, *37*, 785−789.
(43) Lee, T. J.; Jayatilaka, D. *Chem. Phys. Lett.* **1993**, *201*, 1−10.
(44) Lee, T. J.; Rendell, A. P.; Dyall, K. G.; Jayatilaka, D. *J. Chem. Phys.* **1994**, *100*, 7400−7409.
(45) Fletcher, G. D.; Gordon, M. S.; Bell, R. L. *Theor. Chem. Acc.* **2002**, *107*, 57−70.
(46) Aikens, C. M.; Fletcher, G. D.; Schmidt, M. W.; Gordon, M. S. *J. Chem. Phys.* **2006**, *124*, 014107.
(47) Pople, J. A.; Head-Gordon, M.; Raghavachari, K. *J. Chem. Phys.* **1987**, *87*, 5968−5975.
(48) Dunning, T. H. *J. Chem. Phys.* **1971**, *55*, 716−723.
(49) Frisch, M. J.; Pople, J. A.; Binkley, J. S. *J. Chem. Phys.* **1984**, *80*, 3265−3269.
(50) Gonzales, G.; Schlegel, H. B. *J. Chem. Phys.* **1989**, *90*, 2154−2161.
(51) Piecuch, P.; Kucharski, S. A.; Kowalski, K.; Musial, M. *Comput. Phys. Commun.* **2002**, *149*, 71−96.
(52) Piecuch, P.; Wloch, M. *J. Chem. Phys.* **2005**, *123*, 224105.
(53) Schmidt, M. W.; Baldridge, K. K.; Boatz, J. A.; Elbert, S. T.; Gordon, M. S.; Jensen, J. H.; Koseki, S.; Matsunaga, N.; Nguyen, K. A.; Su, S. J.; Windus, T. L.; Dupuis, M.; Montgomery, J. A. *J. Comput. Chem.* **1993**, *14*, 1347−1363.
(54) ACES II is a program product of the Quantum Theory Project, University of Florida. Authors: Stanton, J. F.; Gauss, J.; Perera, S. A.; Yau, A. D.; Watts, J. D.; Nooijen, M.; Oliphant, N.; Szalay, P. G.; Lauderdale, W. J.; Gwaltney, S. R.; Beck, S.; Balkova, A.; Bernholdt, D. E.; Baeck, K.-K.; Rozyczko, P.; Sekino, H.; Huber, C.; Pittner, J.; Bartlett, R. J. Integral packages included are VMOL (J. Almlof and P. R. Taylor), VPROPS (P. Taylor), and ABACUS (T. Helgaker, H. J. Aa. Jensen, P. Jørgensen, J. Olsen, and P. R. Taylor).
(55) Grunenberg, J.; Streubel, R.; Frantzius, G.; Marten, W. *J. Chem. Phys.* **2003**, *119*, 165−169.
(56) Bickelhaupt, F. M.; DeKock, R. L.; Baerends, E. J. *J. Am. Chem. Soc.* **2002**, *124*, 1500−1505.
(57) Seo, Y.; Kim, Y.; Kim, Y. *Chem. Phys. Lett.* **2001**, *340*, 186−193.
(58) Nizkorodov, S. A.; Meuwly, M.; Maier, J. P.; Dopfer, O.; Bleske, E. J. *J. Chem. Phys.* **1998**, *108*, 8964−8975.
(59) Hiraoka, K.; Katsuragawa, J.; Minamitsu, A.; Ignacio, E. W.; Yamabe, S. *J. Phys. Chem. A* **1998**, *102*, 1214−1218.
(60) Gudeman, C. S.; Begemann, M. H.; Pfaff, J.; Saykally, R. J. *J. Chem. Phys.* **1983**, *78*, 5837−5838.
(61) Owrutsky, C.; Gudeman, C. S.; Martner, C. C.; Tack, L. M.; Rosenbaum, N. H.; Saykally, R. J. *J. Chem. Phys.* **1986**, *84*, 605−617.
(62) Kabbadj, Y.; Huet, T. T.; Rehfuss, B. D.; Gabrys, C. M.; Oka, I. *J. Mol. Spectrosc.* **1994**, *163*, 180−205.
(63) Gudeman, C. S.; Saykally, R. J. *Ann. Rev. Phys. Chem.* **1984**, *35*, 387−418.
(64) Herzberg, G.; Huber, K.-P. *Constants of Diatomic Molecules*; Van Nostrand Reinhold: New York, 1979.
(65) Ferguson, J. W.; Dudley, T. J.; Sears, K. C.; Gordon, M. S.; Houk, R. S. submitted to *Spectrochim. Acta, Part B*.
(66) Woods, R. C.; Dixon, T. A.; Saykally, R. J.; Szanto, P. G. *Phys. Rev. Lett.* **1975**, *35*, 1269−1272.
(67) Woods, R. C.; Saykally, R. J.; Anderson, T. G.; Dixon, T. A.; Szanto, P. G. *J. Chem. Phys.* **1981**, *75*, 4256−4260.
(68) Bogey, M.; Demuynck, C.; Destombes, J. L. *Mol. Phys.* **1981**, *43*, 1043−1050.
(69) Sastry, K. V. L. N.; Herbst, E.; De Lucia, F. C. *J. Chem. Phys.* **1981**, *75*, 4169−4170.
(70) Van den Heuvel, F. C.; Dymanus, A. *Chem. Phys. Lett.* **1982**, *92*, 219−222.
(71) Gudeman, C. S.; Begemann, M. H.; Pfaff, J.; Saykally, R. J. *Phys. Rev. Lett.* **1983**, *50*, 727−731.
(72) Wahlgren, U.; Liu, B.; Pearson, P. K.; Schaefer, H. F. *Nature* **1973**, *246*, 4.
(73) Woods, R. C. *Philos. Trans. R. Soc. A* **1988**, *324*, 141.

(74) Woods, R. C. In *Ion and Cluster Ion Spectroscopy and Structure*; Maier, J. P., Ed.; Elsevier: Amsterdam, 1989.
(75) Bouma, W. J.; Burgers, P. C.; Holmes, J. L.; Radom, L. *J. Am. Chem. Soc.* **1986**, *108*, 1767−1770.
(76) Øiestad, Å. M. L.; Uggerud, E. *Int. J. Mass Spectrom. Ion Process* **2000**, *201*, 179−185.
(77) van Mourik, T.; Dunning, T. H.; Peterson, K. A. *J. Phys. Chem. A* **2000**, *104*, 2287−2293.
(78) Gudeman, C. S.; Woods, R. C. *Phys. Rev. Lett.* **1979**, *48*, 1344−1348.
(79) Woods, R. C.; Gudeman, C. S.; Dickman, R. L.; Goldsmith, P. F.; Huguenin, G. R.; Irvine, W. M.; Hjalmarson, Å.; Nyman, L.-Å.; Olofsson, H. *Astrophys. J.* **1983**, *270*, 583.
(80) Blake, G. A.; Helminger, P.; Herbst, E.; De Lucia, F. C. *Astrophys. J.* **1983**, *264*, L69.
(81) Berry, R. J.; Harmony, M. D. *J. Mol. Spectrosc.* **1988**, *128*, 176−194.
(82) Pople, J. A.; Curtiss, L. A. *J. Chem. Phys.* **1991**, *95*, 4385−4388.
(83) Palaudoux, J.; Hochlaf, M. *J. Chem. Phys.* **2004**, *121*, 1782−1789.
(84) Values obtained from NIST Chemistry WebBook at http://webbook.nist.gov/chemistry.
(85) Ruscic, B.; Berkowitz, J. *J. Chem. Phys.* **1991**, *95*, 4033−4039.
(86) Yarkony, D. A. *J. Am. Chem. Soc.* **1992**, *114*, 5406−5411.
(87) Aschi, M.; Harvey, J. N.; Schalley, C. A.; Schröder, D.; Schwarz, H. *Chem. Commun.* **1998**, 531−532.
(88) Harvey, J. N.; Aschi, M. *Phys. Chem. Chem. Phys.* **1999**, *1*, 5555−5563.
(89) Bouma, W. J.; Nobes, R. H.; Radom, L. *Org. Mass Spectrom.* **1982**, *17*, 315.
(90) Curtiss, L. A.; Kock, D.; Pople, J. A. *J. Chem. Phys.* **1991**, *95*, 4040−4043.
(91) Øiestad, Å. M. L.; Uggerud, E. *Int. J. Mass Spectrom. Ion Process* **1997**, *167/168*, 117-126.